On Hamiltonian cycles in the FCC grid
POST-PRINT

Article published on

Computers & Graphics, Vol. 89, 2029, pp.88-93

https://www.sciencedirect.com/science/article/pii/S0097849320300662?via%3Dihub

Lidija Čomić comic@uns.ac.rs
Faculty of Technical Sciences, University of Novi Sad, 21000 Novi Sad, Serbia

Paola Magillo magillo@dibris.unige.it
DIBRIS, University of Genova, 16146 Genova, Italy

Abstract

The face centered cubic (FCC) grid is a space-filling grid, one of the alternatives to the traditional cubic one. We show that there are five Hamiltonian cycles (non-equivalent up to rotation and symmetry), connecting the faces of a voxel in the FCC grid. Each of the five cycles can be used to trace the boundary of a class of objects in the grid, constructed by iteratively attaching voxels so that each new voxel shares exactly one face with the set of already attached voxels.

1 Introduction

A Hamiltonian cycle in a graph G is a cycle that visits every vertex of G exactly once [6]. The problem of finding a Hamiltonian cycle in an arbitrary graph is NP-complete [9]. In this paper we are interested in constructing Hamiltonian cycles for a specific type of graphs, in which the nodes represent the rhombic faces of a voxel in the face centered cubic (FCC) grid, and the arcs represent the (edge-)adjacency relation between them.

An object O in the grid is a finite connected set of voxels. Tracking and displaying the boundary of an object has many applications such as medical imaging or visualization of scientific data sets [7]. For the cubic grid, it has been shown that any of the two Hamiltonian cycles (non-equivalent up to rotation and symmetry) that connect all faces of the cube can be used to define a Hamiltonian cycle on all boundary faces of an object that is obtained starting from a single cube by iteratively attaching cubes so that each newly attached cube shares exactly one face with the already attached ones [10]. Such objects have a tree-like structure: the dual graph $T = (N, A)$ of the object O, which has a node for each cube in O and two nodes in N are connected through an arc in A if the corresponding cubes share a common face, is a tree.

Hamiltonian cycles are of special interest for decomposing a polygonal mesh into triangle strips, which are needed for efficient mesh processing by graphic hardware [14]. They have also been used in computer art [1].

We show that there are five non-equivalent Hamiltonian cycles on the faces of the voxel in the FCC grid, and that each of them can be used to define a Hamiltonian cycle on all boundary faces of a tree-like object O in this grid. Note that a tree-like object in the FCC grid is not necessarily simply connected: it may contain pairs of vertex-adjacent voxels. This parallels our existing work, which considers the same problem on the body-centered cubic (BCC) [3] and the diamond [2] grids.

This paper is organized as follows. In Section 2 we introduce background notions on 3D grids, in Section 3 we review related work, in Section 4 we present our contributions, and in Section 5 we summarize the paper.

2 Non-Traditional 3D Grids

The only regular grid in 3D is the cubic one. Other grids are known from crystallography [8], such as the face centered cubic (FCC), body centered cubic (BCC) or diamond grids, and they receive increasing attention in the literature. Each of these grids has its advantages and drawbacks depending on the application.

The FCC grid is obtained from the cubic one by placing one point at the center of each unit cube, and one point at the center of each of its edges. In the BCC grid, instead, one point is placed at the center and one point at each vertex of the unit cube. In the diamond grid, each point is a center of a tetrahedron, having other four points at the tetrahedron vertices.

The Voronoi diagram of grid points induces a tessellation of the 3D space into voxels. The voxel (3-cell) of the FCC grid is the rhombic dodecahedron (see Figure 1). It has twelve rhombic faces and two types of vertices: open vertices, at the acute (sharp) angles, and closed vertices at the obtuse angles in each rhombic face. Two non-disjoint voxels in the FCC grid either share an entire (rhombic) face or an (open) vertex.

The voxel (3-cell) of the BCC grid is the truncated octahedron, with eight regular hexagonal faces and six square faces (see Figure 2 (a)). Two voxels in the BCC grid are either disjoint or they share an entire (hexagonal or square) face.

The voxel (3-cell) of the diamond grid is the triakis truncated tetrahedron. It has four regular hexagonal faces and twelve isosceles triangular faces (see Figure 2 (b)). There are two types of tetrahedra, depending on the orientation. Two non-disjoint voxels in the diamond grid either share an entire (hexagonal or triangular) face or a vertex. Two tetrahedra sharing a hexagonal face are of the opposite type, as are those sharing only a vertex. Those sharing a triangular face are of the same type.

3 Related Work

In the BCC grid, there is a unique Hamiltonian cycle up to rotation and symmetry, i.e., up to cyclic permutation and permutation of coordinate axes, among those symmetric with respect to the voxel center [3], connecting the faces of the truncated octahedron (see Figure 3). It is obtained through exhaustive search, which is simplified by noticing that in each such cycle, each square face is adjacent to two hexagonal

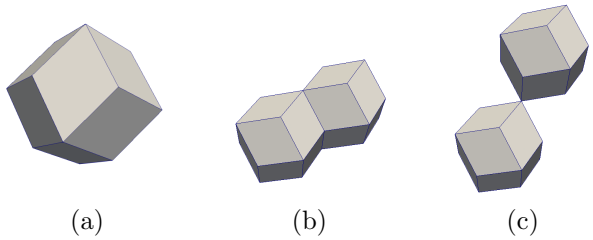

(a) (b) (c)

Figure 1: A voxel of the FCC grid (a). All voxels are congruent through translation. Two non-disjoint voxels share either an entire face (b) or just a vertex (c).

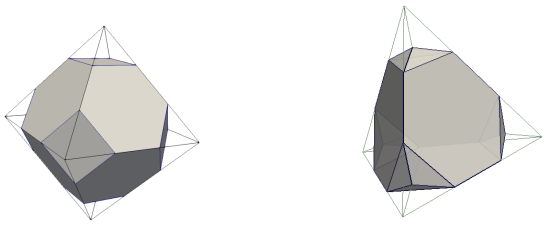

(a) (b)

Figure 2: (a) A voxel of the BCC grid. All voxels in this grid are congruent through translation. (b) A voxel of the diamond grid. There are two types of voxels congruent through translation: the shown one and the one rotated upside down.

faces, and there are exactly two pairs of adjacent hexagonal faces.

In the diamond grid, there are two non-equivalent (oriented) Hamiltonian cycles [2], i.e., only one if the orientation is disregarded (see Figure 4). This cycle is obtained through exhaustive search, which is simplified by noticing that each such cycle visits each face in a group of three triangular faces consecutively,

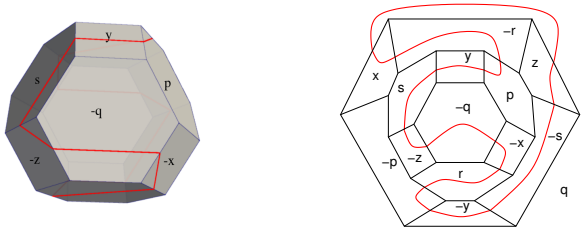

Figure 3: The centrally symmetric Hamiltonian cycle connecting the faces of the BCC voxel (in red). On the right, the voxel surface has been flattened on the plane and one hexagonal face became the unbounded face.

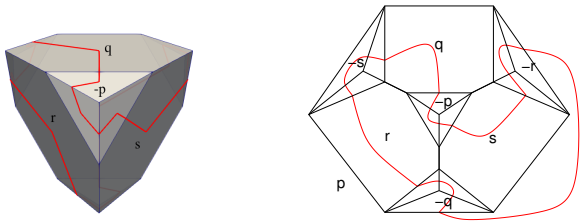

Figure 4: The Hamiltonian cycle connecting the faces of the voxel of the diamond grid. On the right, the voxel surface has been flattened on the plane, and one hexagonal face became the unbounded face.

i.e., the cycle is of the form $H_1T_1H_2T_2H_3T_3H_4T_4$, where H_i is a hexagonal face, and T_i is a group of triangular faces, the first triangular face in the group being adjacent to H_i and the last one being adjacent to H_{i+1} (indexes are taken mod 4).

The cycles in the two grids can be used to define a Hamiltonian cycle (and thus to trace the boundary) on all boundary faces of tree-like objects in these grids, constructed by iteratively attaching the voxels so that each new voxel shares exactly one face with the set of already attached ones [3, 2]. In the diamond grid, the object must be composed of voxels of the same type (attached through one triangular face). Such an object in the diamond grid is necessarily simply connected: two voxels of the same type are never vertex-adjacent.

To our knowledge, no result exists in the literature about non-equivalent Hamiltonian cycles in the FCC grid. The cuboctahedron, which is the dual polyhedron of the FCC voxel (rhombic dodecahedron), is known to be Hamiltonian, but no characterization of non-equivalent cycles was developed.

4 Hamiltonian cycles on the faces of the FCC grid

Each voxel in the FCC grid has twelve rhombic faces, that are in a one-to-one correspondence with the edges of the unit cube (see Figure 5). The Hamiltonian cycle on the faces of the FCC voxel corresponds to a cycle of the cube edges, where each two consecutive edges are adjacent (have a common endpoint).

Proposition 1 *There are five non-equivalent Hamiltonian cycles on the faces of a voxel in the FCC grid.*

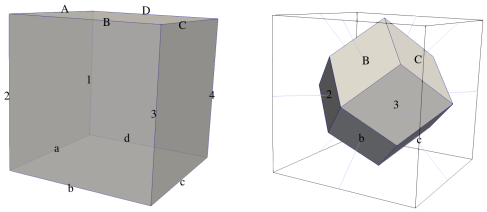

(a) (b)

Figure 5: The cube edges (a) correspond to the faces of the FCC voxel (b).

Proof
A cycle may traverse the four edges of a cube face according to four possible schemes:

(4) all four edges consecutively,

(3+1) three edges consecutively, and one separately,

(2+2) two edges consecutively, and the other two edges consecutively,

(2+1+1) two edges consecutively, and each of the other two edges separately.

Considering the vertices of the cube, a cycle may traverse the three edges incident in a vertex in three possible ways:

[4] all three edges consecutively,

[2+1] two edges consecutively and one separately, or

[1+1+1] all three edges separately.

The proof of Proposition 1 follows from the following three lemmas:

Lemma 1 *There are two non-equivalent Hamiltonian cycles on the faces of the voxel in the FCC grid, traversing some cube face with the scheme (4).*

Lemma 2 *There is one Hamiltonian cycle on the faces of the voxel in the FCC grid, up to equivalence, traversing no face with the scheme (4), and some face with the scheme (3+1).*

Lemma 3 *There are two non-equivalent Hamiltonian cycles on the faces of the voxel in the FCC grid, traversing no face with the scheme (4) or (3+1).*

Since the lemmas cover all possibilities for a Hamiltonian cycle, Proposition 1 follows from them.

The three lemmas will be proven having in mind the four ways for traversing a cube face and the three ways for traversing a cube vertex.

We denote by A, B, C and D the edges on the upper horizontal face of the cube, 1, 2, 3 and 4 the vertical edges and a, b, c and d the edges on the lower horizontal face (see Figure 5). The same symbols denote the corresponding faces of the FCC voxel.

We will form partial paths of cube edges (FCC faces) and consider the possible ways to extend them to Hamiltonian cycles. A necessary condition for completing a partial path to a Hamiltonian cycle is that the set of the remaining edges (i.e., the edges not yet included into the path) forms a single connected component.

Proof of Lemma 1

Without loss of generality, let the upper face of the cube be traversed with the scheme (4), and let the edges of the upper face be traversed as $ABCD$. If this happens for another face, or with the edges of the face traversed in a different sequence, the cycles will be equivalent modulo rotation and symmetry.

From D, it is possible to go either to 1 or to 4. We first consider the case in which the path continues to 1. A path starting with $ABCD1$ can continue to a or d:

- $ABCD1a$ cannot continue to 2 or b, because that blocks the access to A, and the Hamiltonian cycle cannot be completed. Thus, it continues to d, and the obtained cycle is $\mathcal{C}_1^{ABCD} = ABCD1ad4c3b2$.
- $ABCD1d$ cannot continue to a because that blocks access to A, or to c because 4 gets disconnected from $a, b, 2, 3$. Thus, it continues to 4 and the obtained cycle is $\mathcal{C}_2^{ABCD} = ABCD1d4c3ba2$.

Now, we consider the case in which the path continues to 4. $ABCD4$ can continue to d or c.

- $ABCD4d$ cannot continue to 1 or a, because that blocks the access to A, and the Hamiltonian cycle cannot be completed. The obtained cycle is $\mathcal{C}_3^{ABCD} = ABCD4dc3b2a1$.
- $ABCD4c$ cannot continue to d because that blocks access to A, or to b because 3 gets disconnected from $a, d, 1, 2$. Thus, the only possible cycle is $\mathcal{C}_4^{ABCD} = ABCD4c3b2ad1$.

The four cycles are shown in Figure 6.

Looking at Figure 6, we see that C_2^{ABCD} and C_3^{ABCD} traverse two faces with the scheme (4): $ABCD$ and one of its edge-adjacent faces. The two faces adjacent to both such faces are traversed with the scheme (3+1), and the remaining two faces with the scheme (2+1+1). Four vertices are traversed with the scheme [3] and four with the scheme [2+1]. The cycle C_3^{ABCD} is symmetric to C_2^{ABCD} with respect to the plane through the edges 1 and 3.

Still looking at Figure 6, we see that the cycles C_1^{ABCD} and C_4^{ABCD} traverse just one face with the scheme (4), i.e., $ABCD$. The opposite face is traversed with the scheme (2+1+1), two of the remaining faces are traversed with the scheme (2+2) and two with the scheme (3+1); among them, the pairs of faces traversed with the same scheme share an edge. Four vertices are traversed with the scheme [3] and four with the scheme [2+1]. The cycle C_4^{ABCD} is symmetric to C_1^{ABCD} with respect to the plane through the edges 1 and 3.

Thus, the FCC voxel has two classes of Hamiltonian cycles containing the scheme (4). We take C_1^{ABCD} and C_2^{ABCD} as representatives of these two classes.

Proof of Lemma 2

Lemma 2 considers the Hamiltonian cycles traversing three edges of some face consecutively, which have not been considered in Lemma 1, i.e., the ones traversing no face with the scheme (4). Without loss or generality, let the cycle start from the edges ABC.

The cycle can arrive to A from 1 or 2. From C, it can go to 3 or 4. Let us examine all possibilities.

First of all, we consider the cycles arriving to A from 1 and continuing to 3. They are of the form $ABC3...1$. A cycle can arrive to 1 from a, d or D. From 3, it can go to b or c.

- $ABC3b...a1$ is impossible, because 2 gets disconnected from $c, d, 4, D$.
- $ABC3c...a1$ is impossible, because $b, 2$ get disconnected from $d, D, 4$.
- $ABC3b...d1$ is impossible because $a, 2$ get disconnected from $c, D, 4$.
- $ABC3c...d1$ is impossible because $b, a, 2$ get disconnected from $4, D$.
- $ABC3b...D1$ gives the cycle $\mathcal{C}_1^{ABC} = ABC3b2adc4D1$.

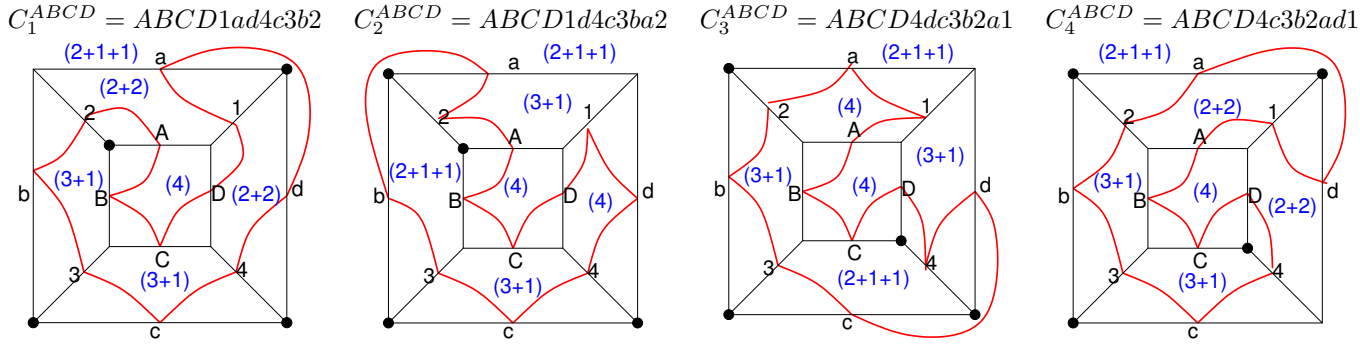

Figure 6: The four cycles starting with the sequence $ABCD$. The cube faces have been flattened on the plane and the lower face $abcd$ is the unbounded part of the plane. Each face is labeled in blue with its traversal scheme, and a cube vertex is marked with a dot if it is traversed with the scheme [3], while it is not marked if it is traversed with the scheme [2+1]. The cycles C_1 and C_4, which traverse just one face with the scheme (4), are mutually equivalent. Similarly, the cycles C_2 and C_3, which traverse two faces with the scheme (4), are mutually equivalent.

- $ABC3c...D1$ gives the cycle $ABC3cb2ad4D1$. But this cycle traverses the four edges of the face $d4D1$ consecutively, thus it has been considered in Lemma 1.

Now, we consider the cycles arriving to A from 1 and continuing to 4, i.e., of the form $ABC4...1$. This is impossible because D gets disconnected from $a, b, c, d, 2, 3$.

Next, we consider the cycles arriving to A from 2 and continuing to 3. They are of the form $ABC3...2$. A cycle can arrive to 2 from a or b. From 3, it can go to b or c.

- $ABC3b...a2$ gives two cycles, $ABC3bc4D1da2$ and $ABC3bcd4D1a2$. They both traverse the face $4D1d$ with the scheme (4), so they have been considered in Lemma 1.

- $ABC3c...a2$ is impossible, because b gets disconnected from $d, D, 1, 4$.

- $ABC3c...b2$ gives two cycles, $ABC3c4D1dab2$ and $ABC3cd4D1ab2$. They traverse the face $C3c4$ with the scheme (4), so they have been considered in Lemma 1.

Finally, we consider the cycles arriving to A from 2 and continuing to 4. They are of the form $ABC4...2$. A cycle can arrive to 2 from a or b. From 4, it can go to c, d or D.

- $ABC4c..a2$ is impossible because $b, 3$ get disconnected from $d, D, 1$.

- $ABC4d..a2$ is impossible because $D, 1$ get disconnected from $b, c, 3$.

- $ABC4D..a2$ gives the cycle $ABC4D1dc3ba2$; this cycle traverses the face $4D1d$ with the scheme (4).

- $ABC4c..b2$ is impossible because 3 gets disconnected from $a, d, 1, D$.

- $ABC4d..b2$ is impossible because $c, 3$ get disconnected from $a, D, 1$.

- $ABC4D...b2$ gives the cycle $\mathcal{C}_2^{ABC} = ABC4D1adc3b2$.

These are all the possibilities with ABC. The two cycles $\mathcal{C}_1^{ABC}$ and $\mathcal{C}_2^{ABC}$ are shown in Figure 7. They traverse four cube faces with the scheme (3+1) and two faces, mutually opposite, with the scheme (2+2). They traverse four cube vertices with the scheme [3], i.e., two opposite vertices of each cube face, and the remaining four vertices with the scheme [2+1].

Looking at Figure 7, we can see that the two cycles are symmetric with respect to the plane through the cube center, orthogonal to the edges B,D, b, d. Equivalently, C_2^{ABC} is the same as C_1^{ABC} starting from the edges $1D4$ instead of ABC. Therefore, there is only one class of cycles containing the scheme (3+1) and not containing the scheme (4). We take $\mathcal{C}_1^{ABC}$ as the representative of this class.

Proof of Lemma 3

Lemma 3 considers those cycles which never traverse more than two edges of a cube face consecutively.

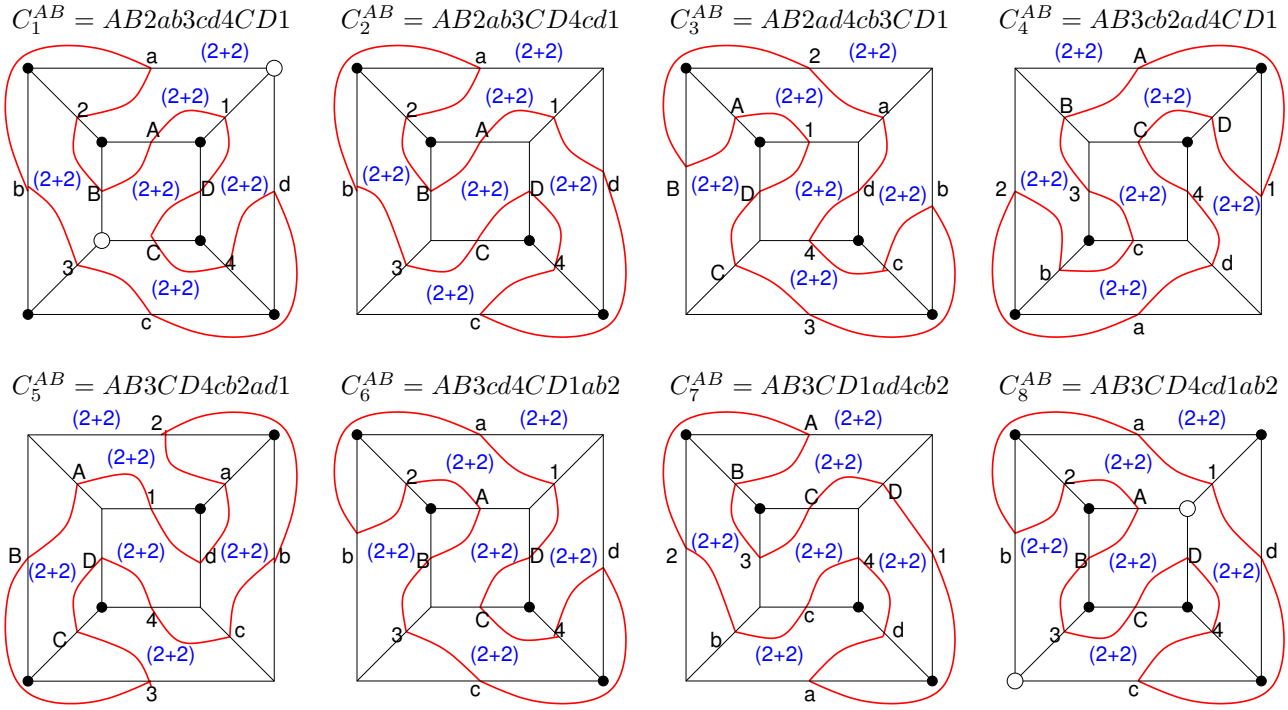

Figure 8: The cycles starting with the sequence AB, not including the ones traversing some face with the scheme (4) of (3+1). They traverse all faces with the scheme (2+2). The cycles in one class (the cycles $\mathcal{C}_1, \mathcal{C}_8$) traverse six vertices consecutively, i.e., all vertices except a pair of opposite ones. The cycles in the other class (all other cycles) traverse four vertices consecutively, which are the endpoints of two opposite cube edges. Vertices are marked according to their traversal scheme: a black dot for the scheme [3], a white dot for the scheme [1+1+1], and no mark for the scheme [2+1].

Let the cycles begin with AB. They can arrive to A from 1 or 2. From B, they can go to 2 or 3.

First, we consider the cycles arriving to A from 1 and continuing to 2. They are of the form $AB2...1$. From 2, the cycle can go to ab, ba, ad or bc.

- $AB2ab..1$ must continue to 3, giving two cycles, $\mathcal{C}_1^{AB} = AB2ab3cd4CD1$ and $\mathcal{C}_2^{AB} = AB2ab3CD4cd1$.
- $AB2ba..1$ and $AB2bc..1$ traverse the face $B2b3$ with the scheme (3+1), thus they have been considered in Lemma 2, and are not considered here.
- $AB2ad..1$ must continue to 4 (and then to cb, and not CD or DC), giving the cycle $\mathcal{C}_3^{AB} = AB2ad4cb3CD1$.

We consider now the cycles arriving to A from 1 and continuing to 3. They are of the form $AB3...1$. From 3, the cycle can go to bc, cb, ba, cd or CD.

- $AB3bc..1$ and $AB3ba..1$ traverse the face $B2b3$ with the scheme (3+1), thus they have been considered in Lemma 2, and are not considered here.
- $AB3cb..1$ must continue to $2ad$, giving the cycle $\mathcal{C}_4^{AB} = AB3cb2ad4CD1$.
- $AB3cd..1$ is impossible because $C, D, 4$ get disconnected from $a, b, 2$.
- $AB3CD..1$ must continue to 4, giving the cycle $\mathcal{C}_5^{AB} = AB3CD4cb2ad1$.

Finally, we consider the cycles arriving to A from 2 and continuing to 3. They are of the form $AB3...2$. From 3, the cycle can go to bc, cb, ba, cd or CD.

- $AB3bc..2$ and $AB3ba..2$ traverse the face $B3b2$ with the scheme (3+1), so they have been considered in Lemma 2.
- $AB3cb..2$ is impossible, because the two vertical edges incident to b are already used.

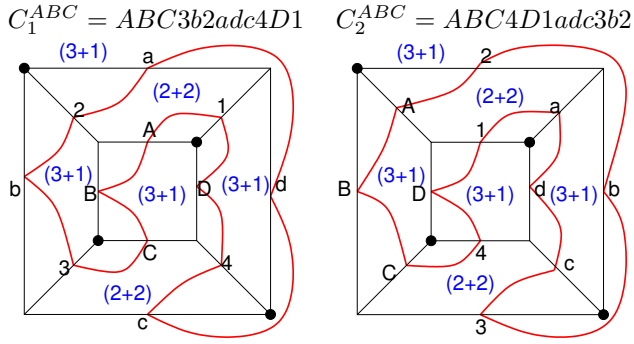

Figure 7: The cycles starting with the sequence ABC, not including the ones traversing some face with the scheme (4). They traverse two opposite faces with the scheme (2+2), the other four faces with the scheme (3+1). They traverse four vertices (marked with a dot) consecutively, i.e., the two opposite vertices of each face. Other (non-marked) vertices are traversed with the scheme [2+1].

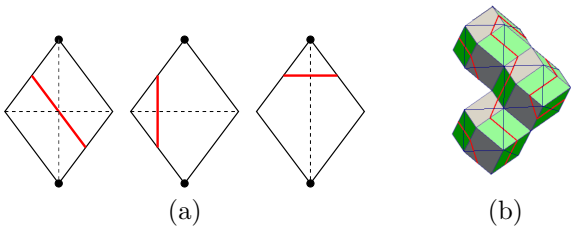

Figure 10: (a) The three ways in which a cycle can traverse a rhombic face (open vertices are marked with a dot), with the corresponding possible triangulations of the face (dotted lines). For a face traversed through two opposite edges (left), we can draw either of the two diagonals. (b) The triangulation of the boundary of a tree-like object O in the FCC grid, induced by a Hamiltonian cycle using individual cycles of the class $\mathcal{C}_2^{AB}$. The green faces could be triangulated with the opposite diagonal as well, the chosen one gives the triangles with better aspect ratio.

- $AB3cd..2$ must continue to 1 or 4. 4 gives the cycle $\mathcal{C}_6^{AB} = AB3cd4CD1ab2$. 1 is impossible, because it disconnects a, b from $4, C, D$.
- $AB3CD..2$ must continue to 1 or 4. 1 gives the cycle $\mathcal{C}_7^{AB} = AB3CD1ad4cb2$, and 4 gives the cycle $\mathcal{C}_8^{AB} = AB3CD4cd1ab2$.

These are all the possibilities with AB. The cycles $\mathcal{C}_i^{AB}$, for $i = 1...8$ are shown in Figure 8. All six faces are traversed with the scheme (2+2).

The cycles $\mathcal{C}_1^{AB}$ and $\mathcal{C}_8^{AB}$ traverse six cube vertices consecutively, i.e., three vertices for each face. The remaining two (diagonally opposite) vertices are traversed with the scheme [1+1+1]. The cycle $\mathcal{C}_8^{AB}$ can be obtained from $\mathcal{C}_1^{AB}$ through symmetry with respect to the horizontal plane through the center of the cube, i.e., through replacing $abcd$ with $ABCD$ and vice versa. Therefore such two cycles are in the same class.

The other six cycles traverse four vertices consecutively, and therefore cannot belong to the same class as $\mathcal{C}_1^{AB}$ and $\mathcal{C}_8^{AB}$. The other four vertices are traversed with the scheme [2+1]. The cycle $\mathcal{C}_4^{AB}$ is the same as $\mathcal{C}_2^{AB}$ starting from the edges $3c$ instead of AB. In the same way, $\mathcal{C}_7^{AB}$ is equal to $\mathcal{C}_2^{AB}$ starting from the edges $C3$. The cycle $\mathcal{C}_6^{AB}$ is symmetric to $\mathcal{C}_2^{AB}$ with respect to the plane passing through the cube center and through the edges 2 and 4. The cycles $\mathcal{C}_3^{AB}$ and $\mathcal{C}_5^{AB}$ are equal to $\mathcal{C}_6^{AB}$ starting from the edges 1D and d1, respectively, instead of AB. Therefore, all cycles $\mathcal{C}_{2..7}$ belong to a unique class.

In conclusion, we have two classes of cycles with AB and not using the scheme (4) or (3+1). We take $\mathcal{C}_1^{AB}$ and $\mathcal{C}_2^{AB}$, respectively, as the representatives of these classes.

The five Hamiltonian cycles $\mathcal{C}_1^{ABCD}, \mathcal{C}_2^{ABCD}, \mathcal{C}_1^{ABC}, \mathcal{C}_1^{AB}$ and $\mathcal{C}_2^{AB}$ represent the five equivalence classes of Hamiltonian cycles, modulo symmetry and rotation. Figure 9 shows the five representative cycles on the FCC voxel. From here on, the representative cycle will be used for denoting the corresponding class as well.

Proposition 2 *There is a Hamiltonian cycle $\mathcal{D}$ on the boundary faces of any tree-like object O in the FCC grid, and $\mathcal{D}$ can be constructed by using just one class of Hamiltonian cycles among $\mathcal{C}_1^{ABCD}, \mathcal{C}_2^{ABCD}, \mathcal{C}_1^{ABC}, \mathcal{C}_1^{AB}, \mathcal{C}_2^{AB}$.*

Proof

The proof is by induction on the number of voxels in O. For a single voxel, the claim is obvious; the Hamiltonian cycle is equal to any member cycle of the selected class, denoted by $\mathcal{C}$.

Let T be the tree of the given tree-like object O, let v be the voxel associated to a leaf node of T, and let O' be the object obtained from O by deleting the voxel v. By induction hypothesis, the thesis holds for O'. Let $\mathcal{D}'$ be the Hamiltonian cycle on the faces of the boundary of O'. Let f be the face shared by the voxel v and the object O'. Note that f is necessarily a boundary face of O', and as such it is in $\mathcal{D}'$.

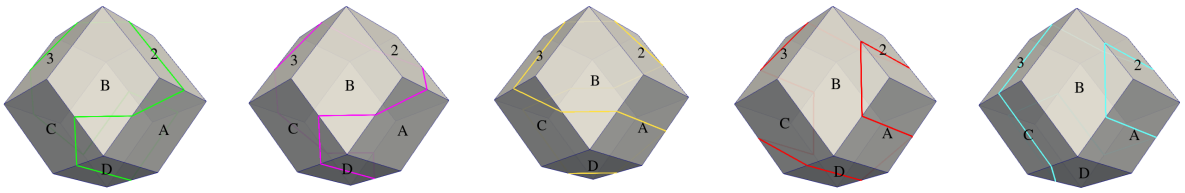

$\mathcal{C}_1^{ABCD} =$ $ABCD1ad4c3b2$ | $\mathcal{C}_2^{ABCD} =$ $ABCD1d4c3ba2$ | $\mathcal{C}_1^{ABC} =$ $ABC3b2adc4D1$ | $\mathcal{C}_1^{AB} =$ $AB2ab3cd4CD1$ | $\mathcal{C}_2^{AB} =$ $AB2ab3CD4cd1$

Figure 9: The five Hamiltonian cycles on the FCC voxel.

The face f is traversed by $\mathcal{D}'$ in one of the three ways (see Figure 10 (a)):

1. through a pair of parallel edges,
2. through a pair of edges adjacent through a closed vertex, or
3. through a pair of edges adjacent through an open vertex.

Recall that open (closed) vertices in the FCC voxel are those with an acute (obtuse) angle in their incident rhombic faces.

In classes $\mathcal{C}_1^{ABCD}, \mathcal{C}_2^{ABCD}, \mathcal{C}_1^{ABC}$, we can find a face traversed in any of the three ways. For example, in the representative cycle $\mathcal{C}_1^{ABCD}$, the face D is traversed through two parallel edges, and the faces A and B through edges adjacent through a closed and an open vertex, respectively. In classes $\mathcal{C}_1^{AB}$, $\mathcal{C}_2^{AB}$, we can find only faces traversed in the first two ways. In any case, the cycle $\mathcal{D}$ is obtained from $\mathcal{D}'$ by replacing the face f with a suitable member (through rotation and/or symmetry) of the same class $\mathcal{C}$ on the voxel v, with f removed.

Figure 11 illustrates the result of Proposition 2. A tree-like object O in the FCC grid is shown, with a Hamiltonian cycle on its boundary, constructed from Hamiltonian cycles on the voxels composing it (in this case, the cycles belonging to the class $\mathcal{C}_2^{AB}$ have been used).

Following the scheme of the proof of Proposition 2, a Hamiltonian cycle on the boundary of a tree-like object can be constructed by choosing an arbitrary cycle for the first voxel, and then incrementally adding face-adjacent voxels with a congruent cycle.

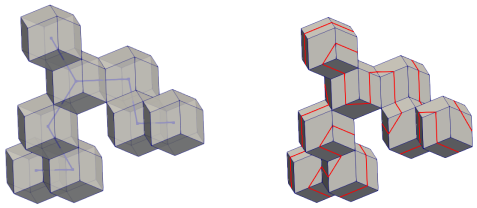

(a) (b)

Figure 11: (a) A tree-like object O in the FCC grid, with the tree T associated with O. (b) A Hamiltonian cycle on the boundary of O. The shown cycle has been obtained by using on individual voxels only the cycles belonging to the class $\mathcal{C}_2^{AB}$.

5 Summary

Beside the classic cubic grid, other three-dimensional grids are gaining attention, among them the BCC grid, the FCC grid and the diamond grid. In this paper, we have characterized the classes of possible Hamiltonian cycles on the faces of the voxel of the FCC grid, i.e., the rhombic dodecahedron. We have also shown that, starting from such cycles, it is always possible to define a Hamiltonian cycle on the surface of any tree-like object in the FCC grid. This work completes our previous results on the BCC and the diamond grids.

Hamiltonian cycles can be used in the generation of triangle strips covering the surface of the object, as well as in efficiently tracing and visualizing the boundary of skeletal shapes.

A Hamiltonian cycle (as the one in Figure 11) naturally induces a generalized triangle strip covering the surface of the tree-like object: each rhombic face traversed through a pair of adjacent edges is triangulated in a unique way (i.e., through the diagonal incident in the common vertex of the two edges), while each rhombic face traversed through a pair of opposite edges can be triangulated in either way (see Figure 10 (a)). Generating triangle strips in this way is much easier than using a generic method for quad-meshes, because we just have to select from a prede-

fined set of cycles (and corresponding face triangulations), for each voxel. The use of the cycles from the classes C_1^{AB} or C_2^{AB} is especially interesting, because all rhombic faces can be triangulated by drawing the shorter diagonal, thus providing a triangulation of good quality (see Figure 10 (b)).

Paths that traverse all faces of a surface are also at the basis of many methods for mesh compression and transmission [15, 13, 12, 4, 16, 18, 5], and Hamiltonian cycles could be considered in this context. Recently, the problem of cutting a polygonal mesh and unfolding it on the plane has gained attention [17, 11]. Such task has applications in manufacturing and packaging. Here, Hamiltonian cycles can be used to obtain a unique band from a mesh.

Acknowledgments

We thank the anonymous reviewers for their useful comments that helped improve the final version of the paper. This work has been partially supported by the Ministry of Education and Science of the Republic of Serbia within the Project No. 34014.

References

[1] E. Akleman, Q. Xing, P. Garigipati, G. Taubin, J. Chen, and S. Hu. Hamiltonian cycle art: Surface covering wire sculptures and duotone surfaces. *Computers & Graphics*, 37(5):316–332, 2013. Special Section on Expressive Graphics.

[2] L. Čomić and P. Magillo. On Hamiltonian Cycles in the Diamond Grid. In *The Third Conference on Mathematics in Engineering: Theory and Applications, Novi Sad*, pages 28–33, 2018.

[3] L. Čomić, P. Magillo, and B. Nagy. On Hamiltonian Cycles in the Body-Centered Cubic Grid. In *The Second Conference on Mathematics in Engineering: Theory and Applications, Novi Sad*, pages 19–23, 2017.

[4] M. Gopi and D. Eppstein. Single-Strip Triangulation of Manifolds with Arbitrary Topology. *Computer Graphics Forum*, 23(3), 2004.

[5] Y. Hao and J.-M. Lien. Compacting Voxelized Polyhedra via Tree Stacking. *Computer Graphics Forum*, 38(7), 2019.

[6] F. Harary. *Graph Theory*. Addison-Wesley, 1969.

[7] G. T. Herman. *Geometry of Digital Spaces*. Birkhauser, Boston, 1998.

[8] C. Kittel. *Introduction to solid state physics*. Wiley, New York, 2004.

[9] J. M. Kleinberg and É. Tardos. *Algorithm design*. Addison-Wesley, 2006.

[10] R. Klette and A. Rosenfeld. *Digital geometry. Geometric methods for digital picture analysis*. Morgan Kaufmann Publishers, San Francisco, Amsterdam, 2004.

[11] E.A. Peraza Hernandez, D.J. Hartl, E. Akleman, and D.C. Lagoudas. Modeling and analysis of origami structures with smooth folds. *Computer-Aided Design*, 78:93–106, 2016.

[12] M. B. Porcu and R. Scateni. An Iterative Stripification Algorithm Based on Dual Graph Operations. In *Eurographics 2003 - Short Presentations*, 2003.

[13] J. Rossignac. Edgebreaker: Connectivity compression for triangle meshes. *IEEE Trans. Vis. Comput. Graph.*, 5(1):47–61, 1999.

[14] G. Taubin. Constructing Hamiltonian Triangle Strips on Quadrilateral Meshes. In H.-C. Hege and K. Polthier, editors, *Third International Workshop "Visualization and Mathematics", VisMath*, Mathematics and Visualization, pages 69–91. Springer, 2002.

[15] G. Taubin and J. Rossignac. Geometric compression through topological surgery. *ACM Trans. Graph.*, 17(2):84–115, 1998.

[16] L. Vása. Optimised mesh traversal for dynamic mesh compression. *Graphical Models*, 73(5):218–230, 2011.

[17] Z. Xi, Y.-H. Kim, Y. J.Kim, and J.-M. Lien. Learning to segment and unfold polyhedral mesh from failures. *Computers & Graphics*, 58:139–149, 2016. Special Issue on SMI 2016.

[18] J. Zhang, C. Zheng, and X. Hu. Triangle mesh compression along the Hamiltonian cycle. *The Visual Computer*, 29(6-8):717–727, 2013.